PHYSICAL REVIEW B VOLUME 22, NUMBER 12 15 DECEMBER 1980

Conduction-band structure of a ferromagnetic semiconductor

W. Nolting
Institute of Physics, University of Würzburg, D-8700 Würzburg, Federal Republic of Germany

A. M. Oleś*
Institute of Physics, Jagellonian University, PL-30-059 Kraków, Poland
(Received 30 May 1980)

We use the s-f model to investigate the energy spectrum, the spectral weights, and the lifetimes of the electronic quasiparticles in a ferromagnetic semiconductor. Starting from two-pole Gaussian *Ansätze* for a complete set of relevant spectral densities and fitting free parameters by exactly calculable spectral moments of these functions, we find a result which reproduces all exactly solvable limiting cases of the s-f model. It is shown that the conduction band splits into several quasiparticle subbands as a consequence of the s-f exchange interaction between conduction electrons and localized magnetic moments. This splitting takes place in principle for all temperatures, i.e., it is not at all due to the onset of ferromagnetism. The spectacular red shifts of the optical absorption edge, observed for EuO, EuS, and EuSe, are almost qualitatively explained by a broadening of the lowest ↑ subband with decreasing temperature.

I. INTRODUCTION

It is well known that typical magnetic semiconductors, as for instance EuO, EuS, $CdCr_2S_4$, and $HgCr_2Se_4$, are well described by the so-called s-f (or d-f, or s-d) model.[1-3] In spite of its very simple nature exact solutions are possible only for some limiting cases.[4,5] The great variety of interesting experiments performed on magnetic semiconductors,[6] however, has challenged a lot of authors to find physically reasonable approaches to the s-f problem using, for instance, perturbation theory,[7,8] canonical transformations,[9,10] Green's-function decoupling,[11] moment techniques,[12-14] and coherent potential approximation (CPA) treatments.[15-17]

For the time being, one of the most exciting problems is the temperature behavior of the conduction-band structure. The striking red shift of the optical absorption edge in cooling below T_c, first observed for the electronic $4f \rightarrow 5dt_{2g}$ transition in the Eu chalcogenides by Busch and Wachter,[18] has found a reasonable explanation by the early perturbation treatment of Rys *et al.*[7] First-order-perturbation theory gives as a result that below T_c the conduction band of a ferromagnetic semiconductor is split into two spin-polarized subbands, the energetic distance of which should be proportional to the magnetization of the system, i.e., should increase with decreasing temperature. The corresponding shift of the lower edge of the stable ↑ subband might then cause the observed red shift. On the other hand, several attempts have been made to exploit this band splitting for constructing a perfect spin filter by use of a EuS-coated tungsten tip.[19-21] The result was a remarkably high degree of spin polarization, being, however, far away from the expected 100%. Similar depolarization effects have been reported by Meier *et al.*[22] for Gd-doped EuO.

These experiments clearly indicate that a spin-polarized splitting of the conduction band must be questioned. One of us proposed therefore a more complex quasiparticle multiband model,[13] which has successfully been applied to the above-mentioned spin-filter experiment.[21] One of the main statements of this model is that the conduction band splits because of the s-f interaction into various quasiparticle subbands, which in general consist of mixed-spin states preventing the electron spin from being totally polarized. The splitting persists in the paramagnetic region $T > T_c$, too. Similar conclusions can be drawn from the CPA calculations.[16,17]

The simplest approach to electronic quasiparticles in the s-f model presented in Ref. 13 is based on a δ-function *Ansatz* for the one-electron spectral density, which leads to correct results in both the atomic and the strong coupling limit. Such an approximation neglects, however, quasiparticle damping (finite lifetimes). So, it may be argued that the derived quasi-particle multiband structure can be only a pecularity of the experimentally uninteresting strong coupling regime. The multiple splitting of the conduction band could indeed become meaningless for moderate coupling constants if the quasiparticle decay were too quick.

It is therefore the aim of this paper to investigate the electronic quasiparticle spectrum of a ferromagnetic semiconductor by taking explicitly into account damping effects and finite lifetimes. It will turn out that the oversimplified first-order-perturbation theory picture that the conduction band splits into two spin-polarized subbands, must be

replaced by an essentially more complicated quasiparticle multiband picture similar to that proposed in Ref. 13. The finite lifetimes of the quasiparticles take care of the fact that for certain values of the system parameters some of the various quasiparticle subbands may be unobservable. That leads, for instance, to an interesting difference in the quasiparticle structure of the conduction band even for such similar materials as EuO and EuS.

In the next section we shortly remind the reader of the s-f model, thereby fixing the notation. In Sec. III we develop the spectral density method for the s-f Hamiltonian (see also Ref. 23). The results are discussed in Sec. IV.

II. s-f MODEL

Typical magnetic semiconductors, as for instance the Eu chalcogenides, have successfully been described within the framework of the s-f model.[1-3] This model attributes the characteristic properties of these substances to a certain spin-spin interaction between two well-defined electronic subsystems. The first is made up by quasifree conduction electrons. H_s is their operator of kinetic energy

$$H_s = \sum_{\vec{k}\sigma} \epsilon(\vec{k})\, a^{\dagger}_{\vec{k}\sigma} a_{\vec{k}\sigma}\,, \tag{2.1}$$

and H_c describes the Coulomb interaction

$$H_c = \tfrac{1}{2} \sum_{\vec{k},\vec{k}',\vec{q};\sigma,\sigma'} v(\vec{q})\, a^{\dagger}_{\vec{k}-\vec{q}\sigma} a^{\dagger}_{\vec{k}'+\vec{q}\sigma'} a_{\vec{k}'\sigma'} a_{\vec{k}\sigma}\,, \tag{2.2}$$

where

$$v(\vec{q}) = \frac{4\pi e^2}{\kappa q^2}\,. \tag{2.3}$$

$a^{\dagger}_{\vec{k}\sigma}$ ($a_{\vec{k}\sigma}$) is the creation (annihilation) operator of an electron with spin σ and wave vector $\vec{k}$. $\epsilon(\vec{k})$ are the energies of the free Bloch band (width W); e is the electron charge and κ the dielectric constant.

The other subsystem consists of strongly localized magnetic moments originating from the electrons of any inner, partially filled atomic shell, which are coupled according to Hund's rule to define the spin operators $\vec{S}_i = (S_i^x, S_i^y, S_i^z)$ acting on the lattice site $\vec{R}_i$. This subsystem is responsible for the magnetism of these materials and is most effectively described by the Heisenberg model

$$H_f = -\sum_{i,j} J_{ij}\, \vec{S}_i \cdot \vec{S}_j\,, \tag{2.4}$$

where J_{ij} are the exchange integrals. In the case of Eu chalcogenides these localized magnetic moments are built up by the seven electrons of the half filled $4f$ shell of the Eu^{2+} ion ($S = \frac{7}{2}$).

Both subsystems are coupled by an intra-atomic exchange interaction H_{sf}

$$H_{sf} = -\frac{g}{2N} \sum_i \sum_{\vec{k},\vec{q}} e^{-i\vec{q}\cdot\vec{R}_i} [S_i^z (a^{\dagger}_{\vec{k}\uparrow} a_{\vec{k}+\vec{q}\uparrow} - a^{\dagger}_{\vec{k}\downarrow} a_{\vec{k}+\vec{q}\downarrow}) + S_i^{+} a^{\dagger}_{\vec{k}\downarrow} a_{\vec{k}+\vec{q}\uparrow} + S_i^{-} a^{\dagger}_{\vec{k}\uparrow} a_{\vec{k}+\vec{q}\downarrow}]\,, \tag{2.5}$$

where g denotes the corresponding s-f coupling constant and $S_j^{\pm} = S_j^x \pm i S_j^y$.

The full s-f model is defined by the sum of the above-introduced partial operators

$$H = H_s + H_c + H_f + H_{sf}\,. \tag{2.6}$$

The many-body problem formulated by this Hamiltonian is far from being solved exactly—approximate solutions are unavoidable.

When treating ferromagnetic semiconductors one has to distinguish between two rather different subjects. The first is that of an empty conduction band, the usual situation for an undoped pure semiconductor at low temperatures, which shall be the subject of this paper. Strictly speaking, we investigate here the energy spectrum of a single electron being excited into an otherwise empty conduction band. In our case the operator H_c (2.2) becomes therefore meaningless.

The other case is that of a partially filled conduction band, which can be achieved by doping with proper impurities [for example, Gd in EuO (Ref. 22)]. Drastic changes in the physical properties of magnetic semiconductors caused by such a doping belong to the most interesting aspects of this field, but are beyond the scope of the present paper.

One of the main difficulties of the s-f problem comes from the Heisenberg term H_f (2.4). On the other hand, however, for the substances of real interest the experiment[6] tells us that typical exchange constants J_{ij} are smaller by some orders of magnitude than typical coupling constants g and typical Bloch bandwidths W. For EuO, e.g., one can assume: $g \simeq 0.2$ eV, $W \simeq 2$ eV, $J_{ij} \lesssim 10^{-3}$ eV. This allows us to find the electronic spectrum of the s-f Hamiltonian (2.6) in two steps. First, we calculate the correlation functions $\langle S_i^{+} S_j^{-} \rangle$ and $\langle S_i^z S_j^z \rangle$ from the Heisenberg Hamiltonian, using the constant coupling approximation (CCA).[24] It means they are calculated from the effective two-spin Hamiltonian with the exchange interaction between the two spins treated exactly and all the other interactions being replaced by the effective fields, proportional to magnetization $\langle S^z \rangle$.[25] This approximation allows us to describe properly the short-range order present in the spin subsystem, which is especially important in the region around T_c. The correlation functions $\langle S_i^{+} S_j^{-} \rangle$ and $\langle S_i^z S_j^z \rangle$ as well as the magnetization $\langle S^z \rangle$ are treated next as pa-

rameters for the electronic problem described by the s-f Hamiltonian (2.6) with $H_f \equiv 0$. Sometimes it is argued that such a neglect of H_f supresses all dependences of the electronic energies on spin-correlation functions as $\langle S_i^+ S_j^- \rangle$ and $\langle S_i^z S_j^z \rangle$. This is of course not true, because these terms appear as a consequence of the s-f interaction part H_{sf} (2.5) even if $H_f \equiv 0$, and only then are they of importance (since $g \gg J_{ij}$).

According to the above arguments we actually work with the following model Hamiltonian

$$\tilde{H} = H_s + H_{sf} \tag{2.7}$$

instead of (2.6). Even with the above simplifications the s-f problem is not exactly solvable.

III. SPECTRAL DENSITY APPROACH

Our approximation is based on the method of spectral moments[12,26,27] which is generally valid for any value of typical model parameters, such as here, temperature T, s-f coupling constant g, and localized spin S. This is certainly an advantage over most of the other approximate procedures.

We start with the on-electron spectral density $A_{\vec{k}\sigma}(\omega)$, which is defined as

$$A_{\vec{k}\sigma}(\omega) = \frac{1}{2\pi} \int_{-\infty}^{+\infty} d(t-t') e^{i\omega(t-t')} \langle [a_{\vec{k}\sigma}(t), a_{\vec{k}\sigma}^{\dagger}(t')]_+ \rangle . \tag{3.1}$$

$[\cdots]_+$ denotes the anticommutator and $\langle \cdots \rangle$ the thermodynamic average. The time-dependent Fermi operators $a_{\vec{k}\sigma}(t)$ and $a_{\vec{k}\sigma}^{\dagger}(t')$ are written in their Heisenberg representation.

We assume that the s-f Hamiltonian $\tilde{H}$ (2.7) possesses a complete and orthonormal system of eigenstates $|n\rangle$ with the eigenenergies E_n

$$H|n\rangle = E_n|n\rangle, \quad \langle n|m\rangle = \delta_{nm} . \tag{3.2}$$

Then it is easy to find the so-called Lehmann representation of the spectral density $A_{\vec{k}\sigma}(\omega)$ by inserting the complete set of eigenfunctions $|n\rangle$ between the two time-dependent operators in Eq. (3.1).

$$A_{\vec{k}\sigma}(\omega) = \frac{1}{Z} \sum_{n,m} |\langle n| a_{\vec{k}\sigma}^{\dagger} |m\rangle|^2 \times e^{-\beta E_n}(1 + e^{-\beta\omega}) \delta(\omega - (E_m - E_n)) . \tag{3.3}$$

Z is the partition function and $\beta = (k_B T)^{-1}$.

The matrix element $\langle n| a_{\vec{k}\sigma}^{\dagger} |m\rangle$ in (3.3) is unequal zero only if the state $|n\rangle$ contains one electron more than the state $|m\rangle$. $|\langle n| a_{\vec{k}\sigma}^{\dagger} |m\rangle|^2$ is then the probability for the excited state

$$|\psi_{m\sigma}(\vec{k})\rangle = a_{\vec{k}\sigma}^{\dagger}|m\rangle = \sum_{p} c_{mp}^{\sigma}(\vec{k}) |p\rangle \tag{3.4}$$

to overlap with the eigenstate $|n\rangle$. The energy differences in the arguments of the δ function in Eq. (3.3) are just the one-electron excitation energies $E_{i\sigma}(\vec{k})$ needed to transfer an additional $(\vec{k}, \sigma)$ electron into the system. Finally, we can write instead (3.3)

$$A_{\vec{k}\sigma}(\omega) = \sum_i \rho_{i\sigma}(\vec{k}) \, \delta(\omega - E_{i\sigma}(\vec{k})) , \tag{3.5}$$

where $\rho_{i\sigma}(\vec{k})$ are positive weight factors with the physical meaning of probability quantities. In a few special cases the sum in (3.5) consists of a finite number of terms only. So, we find for the atomic limit (AL) [$\epsilon(\vec{k}) \equiv T_0 = 0$ for all $\vec{k}$] of the s-f system a two-pole function[17]

$$A_{\sigma}^{\mathrm{AL}}(\omega) = \rho_{1\sigma} \delta(\omega - E_{1\sigma}) + \rho_{2\sigma} \delta(\omega - E_{2\sigma}) , \tag{3.6}$$

$$E_{1\uparrow} = E_{1\uparrow} = -\tfrac{1}{2} gS , \quad E_{2\uparrow} = E_2 = +\tfrac{1}{2} g(S+1) , \tag{3.7}$$

$$\rho_{1\sigma} = \frac{S + 1 + z_\sigma \langle S^z \rangle}{2S+1} , \quad \rho_{2\sigma} = \frac{S - z_\sigma \langle S^z \rangle}{2S+1} , \tag{3.8}$$

$$z_\sigma = \begin{cases} +1 & \text{if } \sigma = \uparrow \\ -1 & \text{if } \sigma = \downarrow \end{cases} . \tag{3.9}$$

For general cases the excited state $|\psi_{m\sigma}(\vec{k})\rangle$ in (3.4) will not be an eigenstate of $\tilde{H}$, possibly possessing an infinite number of nonvanishing coefficients $c_{mp}^{\sigma}(\vec{k})$. With (3.4) in (3.3) we expect then $A_{\vec{k}\sigma}(\omega)$ to be a continuous function of ω. Coming from the atomic limit and also from the strong coupling limit [$g \gg \epsilon(\vec{k})$ for all $\vec{k}$],[4] we have however to assume two pronounced peaks in the $A_{\vec{k}\sigma}(\omega)$ function, the positions and weights of which are to be identified with respective energies and dampings (finite lifetimes) of the two quasiparticles. Elementary many-body theory brings up a Lorentzian shape for the quasiparticle peaks,[28,29] i.e., near the two maxima ($i = 1, 2$) the spectral density $A_{\vec{k}\sigma}(\omega)$ should behave as follows[23]:

$$A_{\vec{k}\sigma}(\omega) \simeq -\frac{1}{\pi} \frac{V_\sigma^{i\,2}(\vec{k}) I_\sigma(\vec{k}, E_{i\sigma}(\vec{k}))}{[\omega - E_{i\sigma}(\vec{k})]^2 + [V_\sigma^{(i)}(\vec{k}) I_\sigma(\vec{k}, E_{i\sigma}(\vec{k}))]^2} , \tag{3.10}$$

where I_σ is the imaginary part of the electronic self-energy $\Sigma_\sigma(\vec{k}, \omega)$

$$I_\sigma(\vec{k}, \omega) = \mathrm{Im}\, \Sigma_\sigma(\vec{k}, \omega) , \tag{3.11}$$

and

$$V_\sigma^{(i)}(\vec{k}) = \left[\left(1 - \frac{\partial}{\partial \omega} \mathrm{Re}\, \Sigma_\sigma(\vec{k}, \omega) \right) \Big|_{\omega = E_{i\sigma}(\vec{k})} \right]^{-1} . \tag{3.12}$$

The Lorentzaian shape of $A_{\vec{k}\sigma}(\omega)$ is however restricted to a small vicinity of the actual peak and holds not at all over the whole ω region, as otherwise the spectral moments $M_{\vec{k}\sigma}^{(\nu)}(A)$, belonging to

$A_{\vec{k}\sigma}(\omega)$

$$M^{(r)}_{\vec{k}\sigma}(A) = \int_{-\infty}^{+\infty} d\omega\, \omega^r A_{\vec{k}\sigma}(\omega) \tag{3.13}$$

$$A_{\vec{k}\sigma}(\omega) = \frac{1}{\sqrt{\pi}} \sum_{i=1}^{2} \frac{\alpha_{i\sigma}(\vec{k})}{[\gamma_{i\sigma}(\vec{k})]^{1/2}} \exp\left(-\frac{[\omega - E_{i\sigma}(\vec{k})]^2}{\gamma_{i\sigma}(\vec{k})}\right). \tag{3.14}$$

This is the main *Ansatz* of our procedure in which the quasiparticle energies $E_{i\sigma}(\vec{k})$, their spectral weights $\alpha_{i\sigma}(\vec{k})$, and the corresponding damping factors $\gamma_{i\sigma}(\vec{k})$ are at first unknown parameters. We fix them by fitting the *Ansatz* (3.14) to the spectral moments $M^{(r)}_{\vec{k}}(A)$ (3.13), which can be calculated independently of the function $A_{\vec{k}\sigma}(\omega)$

$$M^{(r)}_{\vec{k}\sigma}(A) = \langle [([\cdots[[a_{\vec{k}\sigma}, \tilde{H}]_-, \tilde{H}]_-, \ldots, \tilde{H}]_-), \ ([\tilde{H}, \ldots, [\tilde{H}, [\tilde{H}, a^{\dagger}_{\vec{k}\sigma}]_-]_- \cdots]_-)]_+ \rangle, \tag{3.15}$$

where the term in the first set of parentheses on the right-hand side represents $(r-p)$ commutators and the second set encloses p commutators. r and p are integers with $0 \leq p \leq r$. The use of these moments is, however, limited by appearance of certain correlation functions, which cannot be expressed self-consistently by $A_{\vec{k}\sigma}(\omega)$. From (3.15) it is clear that such difficulties will arise for the higher-order moments.

We can avoid these complications by introducing suitable "higher" spectral densities. Similarly to the procedure proposed in Ref. 26 for the Hubbard model, we find such "higher" functions by inspecting the equation of motion

$$[\omega - \epsilon(\vec{k})]\, G_{\vec{k}\sigma}(\omega) = \frac{1}{2\pi} - \frac{1}{2} g z_\sigma [\Gamma_{\vec{k}\sigma}(\omega) + z_\sigma F_{\vec{k}\sigma}(\omega)] \tag{3.16}$$

of the one-electron Green's function $G_{\vec{k}\sigma}(\omega)$, which is connected with $A_{\vec{k}\sigma}(\omega)$ by the relation

$$A_{\vec{k}\sigma}(\omega) = -\frac{1}{\pi} \operatorname{Im} G_{\vec{k}\sigma}(\omega + i0^+). \tag{3.17}$$

We denote with $B_{\vec{k}\sigma}(\omega)$ the higher spectral density which belongs to the static spin function $\Gamma_{\vec{k}\sigma}(\omega)$

$$\Gamma_{\vec{k}\sigma}(\omega) = \frac{1}{N} \sum_{i,j} e^{i\vec{k}\cdot(\vec{R}_i - \vec{R}_j)} \langle\langle S^z_i a_{i\sigma} | a^{\dagger}_{j\sigma} \rangle\rangle, \tag{3.18}$$

and with $C_{\vec{k}\sigma}(\omega)$ the spectral density following from the spin-flip Green's function $F_{\vec{k}\sigma}(\omega)$,

$$F_{\vec{k}\sigma}(\omega) = \frac{1}{N} \sum_{i,j} e^{i\vec{k}\cdot(\vec{R}_i - \vec{R}_j)} \langle\langle S^{-\sigma}_i a_{i-\sigma} | a^{\dagger}_{j\sigma} \rangle\rangle, \tag{3.19}$$

where

$$S^{-\sigma}_i = \begin{cases} S^+_i & \text{if } \sigma = \downarrow \\ S^-_i & \text{if } \sigma = \uparrow \end{cases}. \tag{3.20}$$

This latter function is especially interesting as its poles correspond just to those one-electron excitations which are connected with a simultaneous spin exchange between the excited electron and the localized spin system.

An important feature of the poles of "higher" Green's functions (3.18) and (3.19) is that all must necessarily appear among the poles of $G_{\vec{k}\sigma}(\omega)$, because otherwise the above equation of motion (3.16) could not be fulfilled. This means that for the corresponding spectral densities $B_{\vec{k}\sigma}(\omega)$ [for $\Gamma_{\vec{k}\sigma}(\omega)$] and $C_{\vec{k}\sigma}(\omega)$ [for $F_{\vec{k}\sigma}(\omega)$] such *Ansätze* must be chosen which differ from the *Ansatz* in (3.14) only by the spectral weights:

$$B_{\vec{k}\sigma}(\omega) = \frac{1}{\sqrt{\pi}} \sum_{i=1}^{2} \frac{\beta_{i\sigma}(\vec{k})}{[\gamma_{i\sigma}(\vec{k})]^{1/2}} \exp\left(-\frac{[\omega - E_{i\sigma}(\vec{k})]^2}{\gamma_{i\sigma}(\vec{k})}\right), \tag{3.21}$$

$$C_{\vec{k}\sigma}(\omega) = \frac{1}{\sqrt{\pi}} \sum_{i=1}^{2} \frac{\delta_{i\sigma}(\vec{k})}{[\gamma_{i\sigma}(\vec{k})]^{1/2}} \exp\left(-\frac{[\omega - E_{i\sigma}(\vec{k})]^2}{\gamma_{i\sigma}(\vec{k})}\right). \tag{3.22}$$

We see that the introduction of such a higher spectral density brings along only two new unknown parameters, while there are generally at least three moments of this function, defined quite analogously to Eq. (3.15), which can be determined exactly without the above-mentioned self-consistency problem.

By calculating a sufficient number of A, B, and C moments we get a closed system of equtions to be solved self-consistently. For the reader who is interested in mathematical details we present a concrete calculation in the Appendix.

IV. DISCUSSION OF THE RESULTS

A. Quasiparticle spectrum and red shift of the optical absorption edge

Let us discuss first the energy spectrum of the quasiparticles which is displayed in Fig. 1 for a set of parameters probably realistic for EuS:

$$g = 0.2 \text{ eV}, \quad S = \tfrac{7}{2}, \quad W = 1 \text{ eV}, \quad \text{fcc lattice}. \tag{4.1}$$

The lower (l) and upper (u) edges of the various quasiparticle subbands are plotted as functions of the reduced temperature T/T_c. We see that the conduction band of a ferromagnetic semiconductor splits for each spin direction σ into two quasiparticle subbands. It is important to stress, however, that the spin index ($\uparrow$ or $\downarrow$) of the quasiparticle energies denotes the spin of the electron *before* its

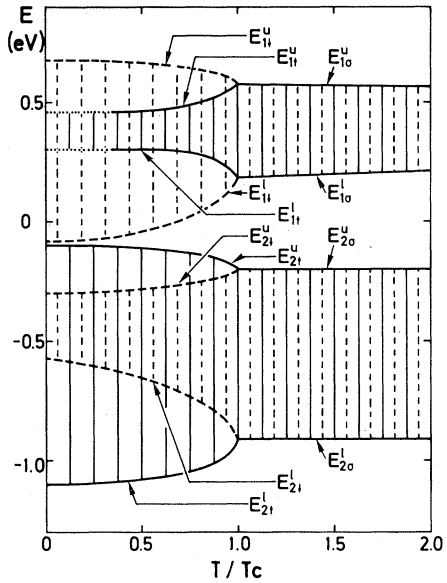

FIG. 1. Lower (l) and upper (u) edges of the quasiparticle subbands as functions of the reduced temperature T/T_c; parameters from Eq. (4.1); solid lines for $\uparrow$ subbands and broken lines for $\downarrow$ subbands.

excitation into such a quasiparticle subband; after the excitation the spin is generally uncertain. These subbands do not at all consist of pure spin states, but rather of complicated mixed-spin states. To understand this let us inspect a special case of the atomic limit[13] taking for simplicity $S=\frac{1}{2}$ for the localized moment. Then the following transitions are possible for a $\uparrow$ electron ($\uparrow e^-$):

$$|\uparrow;0\rangle \xrightarrow{+(\uparrow e^-)} |\uparrow;\uparrow\rangle\,, \tag{4.2}$$

$$|\downarrow;0\rangle \xrightarrow{+(\uparrow e^-)} a|\downarrow;\uparrow\rangle + \beta|\uparrow;\downarrow\rangle\,, \tag{4.3}$$

$$a|\downarrow;\uparrow\rangle - \beta|\uparrow;\downarrow\rangle\,. \tag{4.4}$$

The arrow before the semicolon symbolizes the localized moment (f spin), the entry behind the spin of the electron. Equation (4.2), for example, describes a process where a $\uparrow$-spin electron enters a lattice site with a localized $\uparrow$ spin and no further electron. In the final state the electron spin and f spin are parallel. A spin-flip cannot happen. The final state is therefore a pure spin state. If the $\uparrow$ electron, however, jumps onto a place with a localized $\downarrow$ spin, the final state has to be a mixed-spin state, because electron and localized moment can exchange their spins due to the s-f interaction (2.5). It is easy to derive that there are two such mixed-spin states. Since we have taken $H_f \equiv 0$, the first and the third transitions are degenerated ($-\frac{1}{2}gS$), while the second needs the energy $+\frac{1}{2}g(S+1)$, in accordance with the atomic limit result (3.6) for the one-electron spectral density.

The lower quasiparticle subbands in Fig. 1 are built up by states of the first and third kind [(4.2) and (4.4)]; the upper, by states according to (4.3). So we can expect for $T=0$ only pure spin states (in the lower $\uparrow$ subband), because then the localized spin system is completely aligned, i.e., the initial state $|\downarrow;0\rangle$ of (4.3) and (4.4), respectively, does not occur, and the corresponding transitions cannot be realized.

At this stage we have to point out a possible shortcoming of our procedure. We have taken in (3.14) a two-pole *Ansatz* for the central function $A^{+}_{k\sigma}(\omega)$. This is surely correct in the atomic limit (3.6) because of the mentioned degeneration of the transitions (4.2) and (4.4). This degeneration may however be removed in the finite bandwidth case, so that a three-pole *Ansatz* might be more justified. But both quasiparticle subbands, corresponding to (4.2) and (4.4), will strongly overlap. For the sake of mathematical simplicity we therefore started with the two-pole *Ansatz* (3.14).

Figure 1 shows that the splitting of the conduction band caused by the s-f interaction takes place for all temperatures and not at all only in the ferromagnetic region, as predicted by the perturbation theory.[7,8] For $T>T_c$ $\uparrow$ and $\downarrow$ subbands of course coincide. The temperature dependence of the various quasiparticle subbands manifests itself first of all in bandwidth modifications, especially below T_c. Above T_c this temperature dependence is weak and caused by short-range order in the f subsystem, expressed by the correlation function $\langle \vec{S}_1 \cdot \vec{S}_2 \rangle$. The sharp kink at T_c is only a consequence of the applied CCA[25] and should disappear in a more accurate treatment.

It should be stressed that the result for the temperature dependence of the quasiparticle energies presented in Fig. 1 is quite different from the widely spread opinion that the conduction band of a ferromagnetic semiconductor splits below T_c into two spin-polarized subbands. The splitting seems to be much more complex and does not at all lead to a complete polarization of the electron spin.

The experimentally observed red shift of the optical absorption edge for a suitable electronic transition into the conduction band is explained in our theory by a broadening of a lower $\uparrow$ subband with decreasing temperature. The actual total shift of the lower edge of the conduction band is determined, among others, also by the "free" Bloch bandwidth W. This explains why the Eu chalcogenides EuO, EuS, and EuSe show such different red shifts[6] in spite of the fact that they all have the same lattice structure, the same f-spin value $S=\frac{7}{2}$, and almost the same s-f coupling constant $g \simeq 0.2$ eV, which characterizes a purely intra-atomic interaction of the Eu^{2+} ion. These compounds differ,

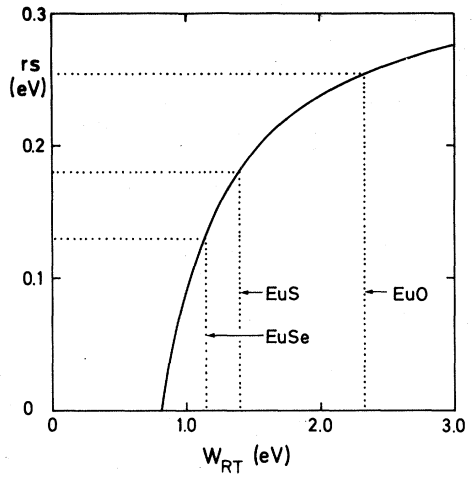

FIG. 2. Total shift of the lower conduction-band edge between room temperature and $T = 0$ K (red shift rs) versus W_{RT}, the conduction bandwidth at room temperature. Indicated are the experimental data for EuO, EuS, and EuSe after Wachter (Ref. 6): rs (EuO) = 0.255 eV, rs (EuS) = 0.18 eV, rs (EuSe) = 0.13 eV. Parameters: fcc lattice, $S = \frac{7}{2}$, $g = 0.2$ eV.

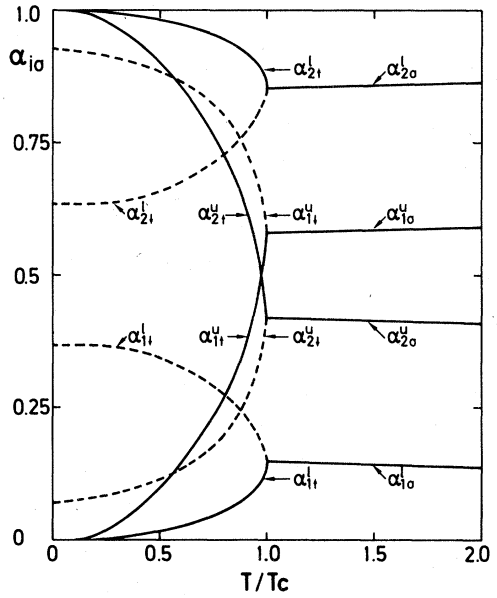

FIG. 3. Temperature dependence of the spectral weights of the various subband edges from Fig. 1 (u, upper edge, l, lower edge, 1, high-energy subband, 2, low-energy subband; solid lines for ↑ subbands, broken lines for ↓ subbands); parameters from Eq. (4.1).

however, by their W values.

In Fig. 2 the total shift of the lower conduction-band edge between room temperature and $T = 0$ K is plotted as a function of W_{RT}, the width of the total conduction band at room temperature. The measured red shifts of the Eu chalcogenides[6] belong to the following values of W_{RT}:

$$W_{RT}(\text{EuO}) = 2.31 \text{ eV}; \quad W_{RT}(\text{EuS}) = 1.40 \text{ eV}; \quad W_{RT}(\text{EuSe}) = 1.15 \text{ eV}. \tag{4.5}$$

The agreement with the values for the experimentally observed $5dt_{2g}$ conduction bandwidth reported by Wachter[6] is very good. The numbers given in (4.5) are also in qualitative agreement with the band-structure calculations of Cho.[30]

B. Spectral weights; finite lifetimes

Up to this point we have discussed only the quasiparticle spectrum, and nothing has been said about spectral weights and finite lifetimes. It may happen that one of the various subbands disappears for certain temperature T or bandwidth W values, because the corresponding spectral weight is zero or too small, or the damping is too big, i.e., the lifetime is too short.

Figure 3 shows the temperature dependence of the spectral weights $\alpha_{i\sigma}(\vec{k})$ for $\vec{k}$ values which belong to the upper u and lower l band edges, respectively. The temperature dependence is essentially strong in the ferromagnetic region (long-range order) while it remains weak only above T_c (due to the spin-spin correlation function $\langle \vec{S}_1 \cdot \vec{S}_2 \rangle$, which reflects the short-range correlations). As already mentioned, the spin-spin correlation function of the localized spin subsystem must be treated in our procedure as input parameter, which has been determined by the CCA.[25] That explains the unphysical kink at T_c.

The high-energy ↑ subband disappears at $T = 0$ because of vanishing spectral weight $\alpha_{1\uparrow}(\vec{k}; T = 0) = 0$. This result is exact since in the ferromagnetic saturation an ↑ electron has its spin parallel to the completely aligned localized spin system, and there cannot be any spin exchange. The ↑ electron therefore moves as a quasifree particle throughout the lattice. The corresponding quasiparticle band is just the free Bloch band, only shifted by an unimportant constant term $-\frac{1}{2}gS$. The ↓ spectrum is of course more complicated because a ↓ electron has, even at $T = 0$, a possibility to create a magnon in the localized spin system, thereby flipping its own spin. The weights of both ↓ subbands are unequal zero. This special case ($T = 0$) is discussed in more detail in Ref. 23. It has been shown also that all the exact results known for the ferromagnetically saturated system[4] are fulfilled by our spectral density approach.

Another interesting result, indicated by Fig. 3, is that all spectral weights have finite values for $T > T_c$. The characteristic splitting of the conduc-

tion band is therefore not at all restricted to the ferromagnetic region but persists for $T > T_c$, too.

The spectral weight curves in Fig. 3 hold for the special set of parameters of Eq. (4.1). Generally, the $\alpha_{i\sigma}(\vec{k})$ are strongly influenced by four variables

$$\alpha_{i\sigma}(\vec{k}) = \alpha_{i\sigma}(\epsilon(\vec{k}), S, W, T), \tag{4.6}$$

the Bloch energy $\epsilon(\vec{k})$, the localized spin S, the width W of the Bloch band, and the temperature T.

Figure 4 shows for two different temperatures, $T = 0.8T_c$ and $T = T_c$, the dependence of $\alpha_{i\sigma}(\vec{k})$ on the bandwidth W, where $\vec{k}$ is chosen according to the lower edges of the quasiparticle subbands. For the $\uparrow$ spectrum the low-energy subband is always stronger weighted than the high-energy one ($\alpha_{2\uparrow} > \alpha_{1\uparrow}$), and with increasing temperature $\alpha_{1\uparrow}$ becomes a bit larger and $\alpha_{2\uparrow}$ smaller (see also Fig. 3). The importance of the higher $\uparrow$ subband decreases monotonically with increasing Bloch bandwidth W. Because of $\alpha_{2\uparrow} = 1 - \alpha_{1\uparrow}$ the weight of the lower $\uparrow$ subband increases on the same scale. The $\downarrow$ weights show an interesting intersection for $T < T_c$. For small widths W the high-energy spectral weight $\alpha_{1\downarrow}$ is larger than the low-energy one ($\alpha_{2\downarrow}$). The point of intersection is temperature dependent, lying for $T = 0$ at $W \simeq 0.8$ eV,[23] and for $T = 0.8T_c$ at $W \simeq 0.46$ eV (Fig. 4). For $T \gtrsim T_c$ the weights do not cross, i.e., $\alpha_{2\sigma} > \alpha_{1\sigma}$ for all W.

From the measured red shifts[6] (see Fig. 1) we can derive the following Bloch bandwidth for the Eu chalcogenides: $W(\mathrm{EuO}) = 2.0$ eV, $W(\mathrm{EuS}) = 0.9$ eV, and $W(\mathrm{EuSe}) = 0.55$ eV. While for EuO the low-energy $\downarrow$ weight $\alpha_{2\downarrow}$ is for all temperatures larger than the high-energy $\downarrow$ weight $\alpha_{1\downarrow}$, the opposite is true for EuS and EuSe for low enough temperatures. This should experimentally be observable in the temperature behavior of the density of states.

As indicated in Eq. (4.6), the $\vec{k}$ dependence of the spectral weights is, strictly speaking, only indirect through the Bloch energies $\epsilon(\vec{k})$. As presented in Fig. 5, the weights are strongly dependent on $\epsilon(\vec{k})$. The ones of the low-energy subbands decrease, when $\epsilon(\vec{k})$ increases from the lower to the upper edge of the Bloch band. The opposite is then true for the weights of the high-energy subbands, which are largest at the upper edge. Note that the curves in Fig. 4 (W dependence) are plotted only for the lower edges, which underestimate the importance of the high-energy quasiparticle subbands. For $W = 1.0$ eV [$\simeq W(\mathrm{EuS})$] we find at $T = 0.8T_c$, according to Fig. 5, $\alpha_{1\uparrow} = 0.055$, $\alpha_{1\downarrow} = 0.275$ at the lower edge, but at the upper edge $\alpha_{1\downarrow} = 0.28$, $\alpha_{1\downarrow} = 0.815$. So, the intersection of the $\alpha_{2\uparrow}(\vec{k})$ and $\alpha_{1\downarrow}(\vec{k})$ curves, for example, is shifted to substantially higher W values, if $\vec{k}$ is taken from the upper edge.

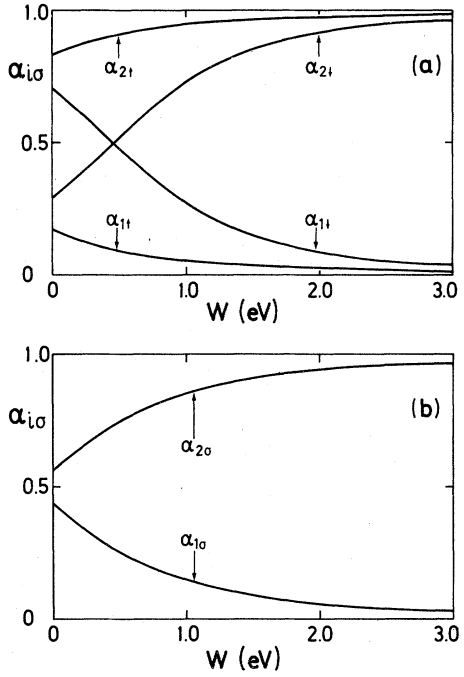

FIG. 4. Spectral weights $\alpha_{i\sigma}(\vec{k})$ for the lower edges of the quasiparticle subbands as functions of the Bloch bandwidth W for two different temperatures; (a) $T = 0.8T_c$, (b) $T = T_c$; 1 corresponds to the high-energy 2, to the low-energy subbands; parameters as in Fig. 2.

To summarize, we present in Table I the general behavior of the various quasiparticle weights as functions of the typical parameters: $T, W, \epsilon(\vec{k}), S$. The S dependence is discussed in the next section. For $T = 0$ we have shown in Ref. 23 that for $S \to \infty$ (classical limit) the lower $\downarrow$ subband will disappear, reproducing the "old" two-band picture.

Let us discuss now the quasiparticle dampings

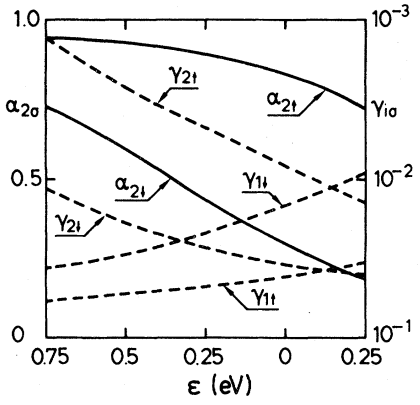

FIG. 5. Spectral weights $\alpha_{i\sigma}$ and damping factors $\gamma_{i\sigma}$ as functions of the Bloch energy ϵ at temperature $T = 0.8T_c$. Parameters are taken from Eq. (4.1); left scale for $\alpha_{i\sigma}$, right scale for $\gamma_{i\sigma}$.

TABLE I. General behavior of the spectral weights and lifetimes of the low- (2) and high- (1) energy quasiparticles as functions of some typical parameters. ↑ means an increase and ↓ a decrease of the weight (lifetime) with increasing parameter.

	$\alpha_{1\uparrow}$	$\alpha_{1\downarrow}$	$\alpha_{2\uparrow}$	$\alpha_{2\downarrow}$	$\tau_{1\uparrow}$	$\tau_{1\downarrow}$	$\tau_{2\uparrow}$	$\tau_{2\downarrow}$
W	↘	↘	↗	↗	↘	↘	↘	↘
ε	↗	↗	↘	↘	↗	↗	↘	↘
$T(<T_c)$	↗	↘	↘	↗	↘	↗	↘	↗
S	↗	↗	↘	↘	↗	↗	↘	↘

$\gamma_{i\sigma}(\vec{k})$, which correspond to finite lifetimes $\tau_{i\sigma} \sim \gamma_{i\sigma}^{-1}$. Figure 6 shows the temperature dependence of $\gamma_{i\sigma}$'s. We see that $\gamma_{2\uparrow} \to 0$ for $T \to 0$, and the corresponding quasiparticle is stable in the ferromagnetic saturation $[\tau_{2\uparrow}(T=0)=\infty]$. $\gamma_{1\uparrow}$ is finite for $T=0$, but the spectral weight $\alpha_{1\uparrow}(T=0)$ is zero, so that we have at $T=0$ only one ↑ subband with stationary quasiparticle. That is, of course, the already discussed simple exact result. The quasiparticles of the lower ↑ subband are always less damped than those of the higher ↑ subband. The trend is not so clear for ↓ subbands. For $W=1$ eV, as in Fig. 6, we still find for all temperatures $\gamma_{2\downarrow} < \gamma_{1\downarrow}$ (i.e., $\tau_{2\downarrow} > \tau_{1\downarrow}$). This can however be changed for smaller W (see Fig. 7) or for smaller spin value S. At $T=0$ $\gamma_{2\downarrow}$ is larger than $\gamma_{1\downarrow}$ for all bandwidths W if $S=\frac{1}{2}$, and for $W \lesssim 0.9$ eV, if $S=\frac{7}{2}$.[23]

Approaching the atomic limit ($W \to 0$) all quasiparticles become stable particles irrespective of S, T, and g. For finite bandwidths W one has to take into consideration their strong dependences on the Bloch energies $\epsilon(\vec{k})$, too. Figure 5 shows that all we have just said about the dampings of ↓ quasi-

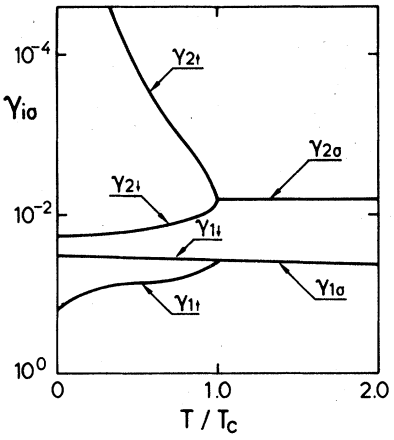

FIG. 6. Temperature dependence of the damping factors $\gamma_{i\sigma}(\vec{k})$. $\vec{k}$ is taken from the lower edges of the various quasiparticle subbands. The other parameters are from Eq. (4.1).

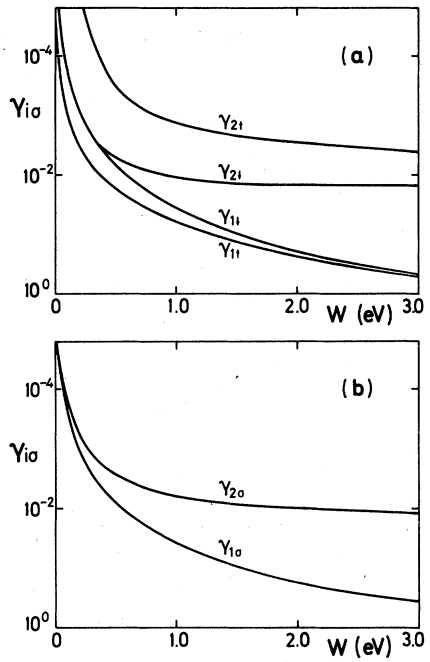

FIG. 7. Damping factors $\gamma_{i\sigma}(\vec{k})$ versus Bloch bandwidth W for two different temperatures: (a) $T=0.8T_c$, (b) $T=T_c$. $\vec{k}$ is taken from the lower edges of the various subbands, other parameters from Eq. (4.1).

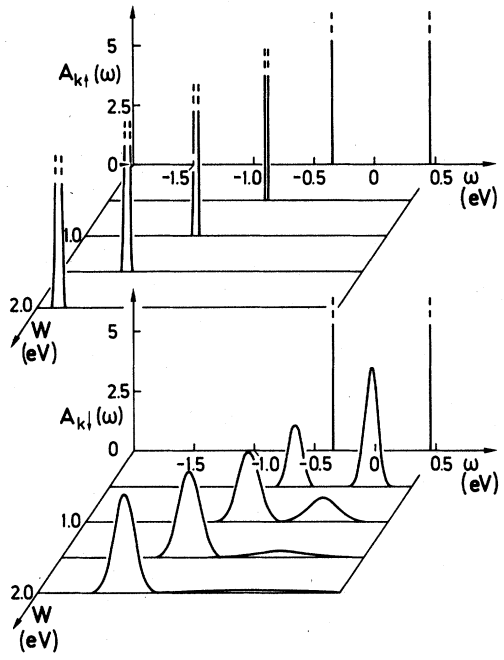

FIG. 8. Spectral densities $A_{\vec{k}\sigma}(\omega)$, $\sigma=\uparrow,\downarrow$, at temperature $T=0.8T_c$ as functions of ω for various values of the Bloch bandwidth W; parameters: $g=0.2$ eV, $S=\frac{7}{2}$, fcc lattice, $\vec{k}$ from the lower band edge.

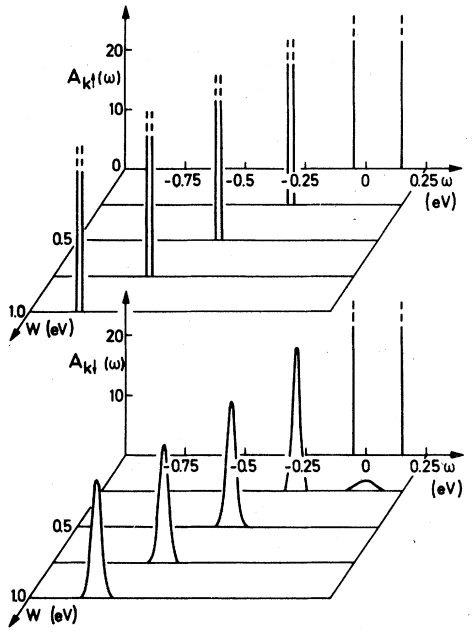

FIG. 9. The same as in Fig. 8 but for $S=\frac{1}{2}$.

particles at the lower edges is quite in contrast to the situation at the upper edges (compare also Figs. 8 and 12). $\gamma_{2\uparrow}$ and $\gamma_{2\downarrow}$ increase with increasing $\epsilon(\vec{k})$, while $\gamma_{1\uparrow}$ and $\gamma_{1\downarrow}$ both decrease.

Combining all these results, we notice that the quasiparticle lifetimes $\tau_{i\sigma}(\vec{k})$ $[\sim\gamma_{i\sigma}^{-1}(\vec{k})]$ depend, analogously as the spectral weights (4.6), on four essential parameters

$$\tau_{i\sigma}(\vec{k}) = \tau_{i\sigma}(\epsilon(\vec{k}), S, W, T). \tag{4.7}$$

The general trends are summarized in Table I. For all parameters we find that $\tau_{2\uparrow} > \tau_{2\downarrow}$ for $T < T_c$, because the ↑ quasiparticle suffers less spin scattering than the ↓ quasiparticle in the partially aligned localized spin system. On the other hand, it is always $\tau_{1\uparrow} < \tau_{1\downarrow}$ for $T < T_c$. This becomes clear with (4.3), because an ↑ electron needs a spin deviation (magnon) in the localized spin system to create a quasiparticle of the higher sub-

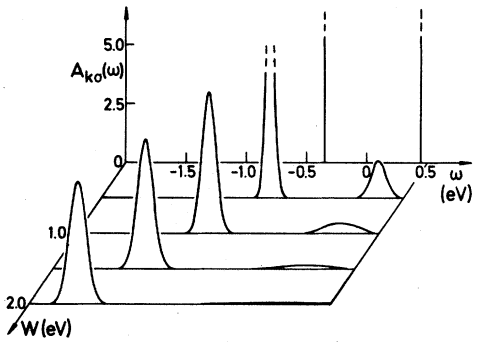

FIG. 10. The same as in Fig. 8 but for $T=T_c$.

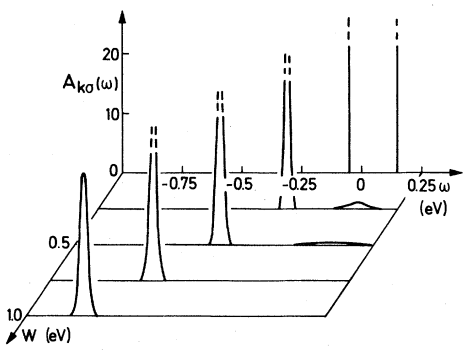

FIG. 11. The same as in Fig. 8 but for $S=\frac{1}{2}$ and $T=T_c$.

band, while a ↓ electron must only be able to emit a magnon, which is, however, always possible.

C. Quasiparticle structure of the spectral density

All the facts which we have derived and discussed in the two preceding sections for the quasiparticle energies $E_{i\sigma}(\vec{k})$, their spectral weights $\alpha_{i\sigma}(\vec{k})$, and their dampings $\gamma_{i\sigma}(\vec{k})$ determine the general shape of the one-electron spectral density $A_{\vec{k}\sigma}(\omega)$ (3.14). Figures 8 to 12 show a few typical examples.

In the atomic limit ($W=0$) our procedure reproduces the exact two-pole function (3.6) for both spin directions and all temperatures $T \neq 0$. For finite bandwidths we observe a distinct quasiparticle structure of the spectral density, where for $T=0.8T_c$ ($S=\frac{7}{2}$ in Fig. 8, $S=\frac{1}{2}$ in Fig. 9) the lower-edge quasiparticles of the upper ↑ subband are to

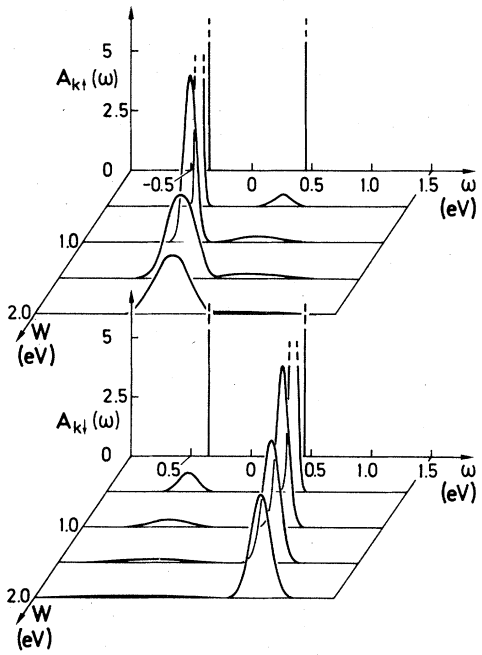

FIG. 12. The same as in Fig. 8, but for a $\vec{k}$ value from the upper edge of the Bloch band.

be seen only for a very small W. These of the lower $\uparrow$ subband have essentially longer lifetimes. The quasiparticles of the upper $\uparrow$ band gain in importance with increasing temperature (Figs. 10 and 11) and with increasing Bloch energy $\epsilon(\vec{k})$ (Fig. 12). In the $\downarrow$ spectrum the quasiparticles of the upper subband are at first more stable than those of the lower subband, if W and T are small enough. This changes with increasing temperature and increasing bandwidth. $\downarrow$ quasiparticles of the higher subband are the better defined the higher the f spin S. The opposite is true for the $\downarrow$ quasiparticles of the lower subband, which completely disappear for $S \to \infty$.

V. CONCLUSIONS

We have presented in this paper an approach to the quasiparticle spectrum of the s-f model for a ferromagnetic semiconductor which takes explicitly into account quasiparticle damping by a Gaussian *Ansatz* for the one-electron spectral density. The credibility of this approach is strongly supported by the exactly solvable limiting cases of the s-f model,[4] which are correctly reproduced without exception.

A further control for more general cases can be drawn from the second spectral moment of the higher spectral density $B_{\vec{k}\sigma}(\omega)$, defined in Eq. (3.21), which has not been used in the actual derivation of our results. The relative error Δ in this moment (A29) is surprisingly never larger than 1.0%, as seen in Fig. 13.

The energies, spectral weights, and dampings of the sf quasiparticles are shown to depend strongly on four parameters, namely, the ratio W/g of Bloch bandwidth W to s-f coupling constant g, the spin S of the localized magnetic moments, the temperature T, and the Bloch energy $\epsilon(\vec{k})$. As a consequence of the s-f exchange interaction, the conduction band of a ferromagnetic semiconductor splits into several quasiparticle subbands, which are characterized by different spectral weights and different lifetimes. The splitting is independent of the onset of ferromagnetism in contrast to the statements of previous methods. The temperature dependence of the quasiparticle subbands manifests itself first of all in modifications of the widths of various subbands. The increasing width of the lowest $\uparrow$ subband leads to the famous red shift of the optical absorption edge. The red shifts that we have calculated are in satisfactory agreement with the experimental data. Thus, in spite of a great deal of simplification, the theory presented here should at least qualitatively describe the conduction-band structure in ferromagnetic semiconductors.

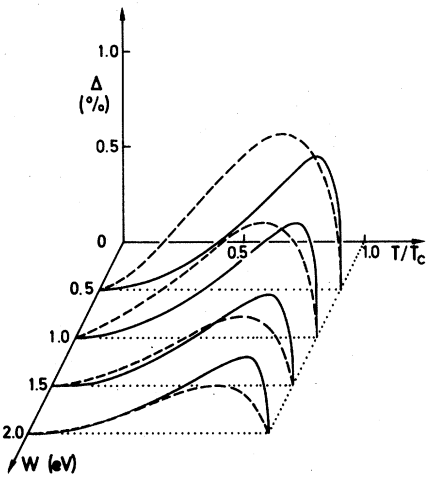

FIG. 13. Relative error $\Delta_{\vec{k}\sigma}$ (A29) in the second moment of the static spin spectral density $B_{\vec{k}\sigma}(\omega)$ (3.21) as a function of T/T_c for various bandwidths W. Parameters: $S=\frac{1}{2}$, $g=0.2$ eV, $\vec{k}$ from the lower band edge of the Bloch band; solid lines for $\sigma=\uparrow$, broken lines for $\sigma=\downarrow$.

APPENDIX

We perform in this Appendix a concrete evaluation of the general spectral density approach presented in Sec. III. The following abbreviations will be used:

$$m = \langle S^z \rangle , \tag{A1}$$

$$D_2 = S^2 - m^2 , \tag{A2}$$

$$D_{1\sigma} = S - z_\sigma m , \tag{A3}$$

$$D_\sigma = D_2 + D_{1\sigma} , \tag{A4}$$

$$\gamma_0^\sigma = \langle S_i^{-\sigma} S_i^\sigma \rangle , \tag{A5}$$

$$R_0 = \langle (S^z)^2 \rangle = S^2 + D_{1\sigma} - \gamma_0^\sigma , \tag{A6}$$

$$S_{0\sigma} = R_0 + \gamma_0^\sigma = S^2 + D_{1\sigma} , \tag{A7}$$

$$\gamma_1^\sigma = \langle S_i^{-\sigma} S_j^\sigma \rangle , \tag{A8}$$

$$R_1 = \langle S_i^z S_j^z \rangle , \tag{A9}$$

$$S_{1\sigma} = R_1 + \gamma_1^\sigma , \tag{A10}$$

$$c_1 = \begin{cases} \frac{1}{24} & \text{for sc lattice} \\ \frac{1}{64} & \text{for bcc lattice} \\ \frac{3}{64} & \text{for fcc lattice} , \end{cases} \tag{A11}$$

$$\eta_{\vec{k}\sigma} = \epsilon(\vec{k}) - \tfrac{1}{2} g z_\sigma m . \tag{A12}$$

On applying Eq. (3.15) we get the following spectral moments of the spectral density $A_{\vec{k}\sigma}(\omega)$:

$$M_{\vec{k}\sigma}^{(0)}(A) = 1 , \tag{A13}$$

$$M_{\vec{k}\sigma}^{(1)}(A) = \eta_{\vec{k}\sigma} , \tag{A14}$$

$$M_{\vec{k}\sigma}^{(2)}(A) = \eta_{\vec{k}\sigma}^2 + \tfrac{1}{4} g^2 D_\sigma , \tag{A15}$$

$$M^{(3)}_{\vec{k}\sigma}(A) = \eta^{3}_{\vec{k}\sigma} + \tfrac{1}{4}g^2\epsilon(\vec{k})(2D_\sigma - m^2 + S_{1\sigma}) + \tfrac{1}{8}g^3[(S+1)D_{1\sigma} - z_\sigma m D_2]\,, \tag{A16}$$

$$\begin{aligned} M^{(4)}_{\vec{k}\sigma}(A) = {} & \eta^{4}_{\vec{k}\sigma} + \tfrac{1}{4}g^2\epsilon^2(\vec{k})[3D_\sigma + 2(S_{1\sigma} - m^2)] + \tfrac{1}{4}g^2 c_1 w^2(S_{0\sigma} - m^2) \\ & + \tfrac{1}{8}g^3\epsilon(\vec{k})[S(S+1)(1-4z_\sigma m) - z_\sigma m(1-4m^2) + S_{0\sigma} + 2S_{1\sigma}] \\ & + \tfrac{1}{16}g^4\{S(S+1)[S(S+1) - 2z_\sigma m] + S_{0\sigma} - m^4\}\,. \end{aligned} \tag{A17}$$

W is the width of the unperturbed Bloch band. The magnetization $m = \langle S^z \rangle$, as well as the correlation functions $\gamma_0^\sigma, \gamma_1^\sigma, R_1$ of the localized spin system are taken as input parameters, predetermined by the cluster approximation of Ref. 25.

The moments of the spectral density $B_{\vec{k}\sigma}(\omega)$ (3.21) obey the following relations:

$$M^{(0)}_{\vec{k}\sigma}(B) = m\,, \tag{A18}$$

$$M^{(1)}_{\vec{k}\sigma}(B) = m\epsilon(\vec{k}) - \tfrac{1}{2}gz_\sigma R_0\,, \tag{A19}$$

$$\begin{aligned} M^{(2)}_{\vec{k}\sigma}(B) = {} & m\epsilon^2(\vec{k}) - \tfrac{1}{2}gz_\sigma\epsilon(\vec{k})(R_0 + R_1) \\ & + \tfrac{1}{4}g^2[S(S+1)m - z_\sigma R_0]\,. \end{aligned} \tag{A20}$$

For the moments of the spin-flip spectral density $C_{\vec{k}\sigma}(\omega)$ (3.22), we get finally

$$M^{(0)}_{\vec{k}\sigma}(C) = 0\,, \tag{A21}$$

$$M^{(1)}_{\vec{k}\sigma}(C) = -\tfrac{1}{2}g\gamma_0^\sigma\,, \tag{A22}$$

$$M^{(2)}_{\vec{k}\sigma}(C) = -\tfrac{1}{4}g^2\gamma_0^\sigma - \tfrac{1}{2}g\epsilon(\vec{k})(\gamma_0^\sigma + \gamma_1^\sigma)\,. \tag{A23}$$

With the *Ansatz* (3.14) inserted into (3.13) we find the following equivalent expressions for the A moments (A13)–(A17):

$$\mathfrak{M}^{(0)}_{\vec{k}\sigma}(A) = \sum_{i=1}^{2}\alpha_{i\sigma}(\vec{k})\,, \tag{A24}$$

$$\mathfrak{M}^{(1)}_{\vec{k}\sigma}(A) = \sum_{i=1}^{2}\alpha_{i\sigma}(\vec{k})\,E_{i\sigma}(\vec{k})\,, \tag{A25}$$

$$\mathfrak{M}^{(2)}_{\vec{k}\sigma}(A) = \sum_{i=1}^{2}\alpha_{i\sigma}(\vec{k})[E^2_{i\sigma}(\vec{k}) + \tfrac{1}{2}\gamma_{i\sigma}(\vec{k})]\,, \tag{A26}$$

$$\mathfrak{M}^{(3)}_{\vec{k}\sigma}(A) = \sum_{i=1}^{2}\alpha_{i\sigma}(\vec{k})[E^3_{i\sigma}(\vec{k}) + \tfrac{3}{2}\gamma_{i\sigma}(\vec{k})E_{i\sigma}(\vec{k})]\,, \tag{A27}$$

$$\mathfrak{M}^{(4)}_{\vec{k}\sigma}(A) = \sum_{i=1}^{2}\alpha_{i\sigma}(\vec{k})[E^4_{i\sigma}(\vec{k}) + 3\gamma_{i\sigma}(\vec{k})E^2_{i\sigma}(\vec{k}) + \tfrac{3}{4}\gamma^2_{i\sigma}(\vec{k})]\,. \tag{A28}$$

Similar expressions hold for the B and C moments. We have only to replace the spectral weights $\alpha_{i\sigma}(\vec{k})$ by $\beta_{i\sigma}(\vec{k})$ and $\delta_{i\sigma}(\vec{k})$, respectively.

We have used the A moments and the C moments to determine the energies $E_{i\sigma}(\vec{k})$, the spectral weights $\alpha_{i\sigma}(\vec{k})$, and the dampings $\gamma_{i\sigma}(\vec{k})$ presented in Sec. IV. The remaining B moments may be then used as an accuracy test of our procedure. Thus we define the relative error $\Delta_{\vec{k}\sigma}$ of the second B moment when calculated with the model spectral density

$$\Delta_{\vec{k}\sigma} = \frac{\mathfrak{M}^{(2)}_{\vec{k}\sigma}(B) - M^{(2)}_{\vec{k}\sigma}(B)}{M^{(2)}_{\vec{k}\sigma}(B)}\,. \tag{A29}$$

*Present address: Max-Planck-Institut für Festkörperforschung, Postfach 800665, D-7000 Stuttgart 80, Federal Republic of Germany.

[1] S. Methfessel and D. C. Mattis, in *Handbuch der Physik. Encyclopedia of Physics*, edited by H. F. Wijn (Springer, New York, 1968), Vol. 18 (1), p. 389.
[2] O. Krisement, J. Magn. Magn. Mater. 3, 7 (1976).
[3] W. Nolting, Phys. Status Solidi B 96, 11 (1979).
[4] W. Nolting, J. Phys. C 12, 3033 (1979).
[5] Y. A. Izyumov and M. V. Medvedev, Z. Eksp. Teor. Fiz. 59, 553 (1970) [Sov. Phys.–JETP 32, 302 (1971)].
[6] For a review concerning the Eu chalcogenides see, P. Wachter, *Handbook on the Physics and Chemistry of Rare Earths*, edited by K. A. Gschneidner and L. Eyring (North-Holland, Amsterdam, 1979), Vol. I, Chap. 19.
[7] F. Rys, J. S. Helman, and W. Baltensperger, Phys. Kondens. Mater. 6, 105 (1967).
[8] C. Haas, Phys. Rev. 168, 531 (1968).
[9] A. Aldea and E. Teleman, J. Phys. C 7, 1491 (1974).
[10] A. Aldea and E. Teleman, Z. Phys. B37, 135 (1980).
[11] R. B. Woolsey and R. M. White, Phys. Rev. B 1, 4474 (1970).
[12] W. Nolting, Phys. Status Solidi B 79, 573 (1977).
[13] W. Nolting, J. Phys. C 11, 1427 (1978).
[14] V. Capek and P. Chvosta, Phys. Status Solidi B 97, 221 (1980).
[15] A. Rangette, A. Yanase, and J. Kübler, Solid State Commun. 12, 171 (1973).
[16] K. Kubo, J. Phys. Soc. Jpn. 36, 32 (1974).
[17] W. Nolting and A. M. Oleś, J. Phys. C 13, 823 (1980).
[18] G. Busch and P. Wachter, Phys. Kondens. Mater. 5, 232 (1966).
[19] N. Müller, W. Eckstein, W. Heiland, and W. Zinn, Phys. Rev. Lett. 29, 1651 (1972).
[20] E. Kisker, G. Baum, A. H. Mahan, W. Reith, and B. Reihl, Phys. Rev. B 18, 2256 (1978).
[21] W. Nolting and B. Reihl, J. Magn. Magn. Mater. 10, 1 (1979).
[22] F. Meier, P. Zürcher, and E. Kaldis, Phys. Rev. B 19, 4570 (1970).
[23] W. Nolting and A. M. Oleś, J. Phys. C 13, 2295 (1980).
[24] P. W. Kasteleijn and J. van Kranendonk, Physica (Utrecht) 22, 317 (1956).

[25]For more details see A. M. Oleś, Phys. Status Solidi B 99, K67 (1980).
[26]W. Nolting, Z. Phys. 255, 25 (1972).
[27]O. K. Kalashnikov and E. S. Fradkin, Phys. Status Solidi B 59, 9 (1973).
[28]A. L. Fetter and J. D. Walecka, *Quantum Theory of Many-Particle Systems* (McGraw-Hill, New York, 1971).
[29]N. M. Hugenholtz, in *Quantum Theory of Many Body Systems*, Many Body Problems, edited by S. F. Edwards (Benjamin, New York, 1969), p. 187.
[30]S. J. Cho, Phys. Rev. B 1, 4589 (1970).